Nuclear Engineering and Technology 54 (2022) 1471–1481

Contents lists available at ScienceDirect

Nuclear Engineering and Technology

journal homepage: www.elsevier.com/locate/net

Original Article

A novel analytical solution of the deformed Doppler broadening function using the Kaniadakis distribution and the comparison of computational efficiencies with the numerical solution

Willian V. de Abreu*, Aquilino S. Martinez, Eduardo D. do Carmo, Alessandro C. Gonçalves

Nuclear Engineering Program - PEN/COPPE-Universidade Federal do Rio de Janeiro, Brazil

ARTICLE INFO

Article history:
Received 20 July 2021
Received in revised form
29 September 2021
Accepted 5 October 2021
Available online 12 October 2021

Keywords:
Deformed Doppler broadening function
Generalized voigt functions
Kaniadakis distribution
Computational efficiencies

ABSTRACT

This paper aims to present a new method for obtaining an analytical solution for the Kaniadakis Doppler broadening (KDB) function. Also, in this work, we report the computational efficiencies of this solution compared with the numerical one. The solution of the differential equation achieved in this paper is free of approximations and is, consequently, a more robust methodology for obtaining an analytical representation of ψ_k. Moreover, the results show an improvement in efficiency using the analytical approximation, indicating that it may be helpful in different applications that require the calculation of the deformed Doppler broadening function.

© 2021 Korean Nuclear Society, Published by Elsevier Korea LLC. This is an open access article under the CC BY-NC-ND license (http://creativecommons.org/licenses/by-nc-nd/4.0/).

1. Introduction

Over the years, several theories have been developed in the field of statistical mechanics and kinetic theory. Most of them start from the assumption of a specific form of entropy: the Boltzmann–Gibbs–Shannon theory, which, in turn, leads to the Maxwell-Boltzmann exponential distribution [1,2].

Despite this, it is known that the Maxwell-Boltzmann statistic and its standard exponential function cannot describe relativistic phenomena of particle systems adequately like, for instance, the case of the cosmic rays flux in a given energy range and the density of rain events versus the event size [3].

Within this context, the Kaniadakis, or κ-deformed statistic, was developed. It is a non-extensive generalization of the ordinary Boltzmann–Gibbs–Shannon (BGS) mechanics statistics based on the kinetical interaction principle (KIP). This new distribution presents the parameter κ, expressing the level of deformation regarding the standard statistic. Hence, when κ tends towards zero, the expression returns to BGS mechanics.

According to Kaniadakis [3], the deformation parameter κ emerges naturally within Einstein's special relativity, implying that this term is a purely relativistic effect. In this context, the author determined the value of κ within the special relativity context as

$$\frac{1}{\kappa^2} = 1 + \left(\frac{mc^2}{k_B T}\right)^2, \tag{1}$$

where T is the temperature of the system, k_B the Boltzmann constant, m the rest mass of the particles, and c light speed.

When considering a relativistic particle systems problem, assuming a nonexponential distribution function with power law tails is necessary. In order to do that, a generalization of the Boltzmann–Gibbs–Shannon distribution is needed. Consequently, it is also required to replace the ordinary exponential function applied in the standard distribution by a one-parameter generalized exponential, $\exp_\kappa$, which is given by Ref. [4]:

$$\exp_\kappa(x) \equiv \left(\sqrt{1+\kappa^2 x^2} + \kappa x\right)^{1/\kappa}, \tag{2}$$

and which obeys the following condition [4]:

$$\exp_\kappa(x) \cdot \exp_\kappa(-x) = 1. \tag{3}$$

One of the possible applications of this new theory is to consider an also new deformed statistical κ-distribution. It can be represented, for instance, in terms of the nuclei velocities in a nuclear reactor [5–7]:

* Corresponding author. Nuclear Engineering Program - PEN/COPPE-Universidade Federal do Rio de Janeiro, Brazil.
E-mail address: wabreu@coppe.ufrj.br (W.V. de Abreu).

https://doi.org/10.1016/j.net.2021.10.003
1738-5733/© 2021 Korean Nuclear Society, Published by Elsevier Korea LLC. This is an open access article under the CC BY-NC-ND license (http://creativecommons.org/licenses/by-nc-nd/4.0/).

$$f_\kappa(V,T) = A(\kappa)\exp_\kappa\left(-\frac{MV^2}{2k_BT}\right), \tag{4}$$

where M is the nucleus mass, V is the velocity of the target nucleus, T is the temperature of the medium and $A(\kappa)$ is defined as:

$$A(\kappa) = \left(\frac{|\kappa|M}{\pi k_B T}\right)^{n/2}\left(1+\frac{3|\kappa|}{2}\right)\frac{\Gamma\left(\frac{1}{2|\kappa|}+\frac{3}{4}\right)}{\Gamma\left(\frac{1}{2|\kappa|}-\frac{3}{4}\right)}. \tag{5}$$

Consequently, with this generalized quasi-Gaussian statistics, it is possible to describe phenomena that may not be accurately described using Maxwell–Boltzmann statistics, such as the physical phenomena outside thermal equilibrium [5] and systems with long-term time correlations [8].

In recent years, Kaniadakis deformed statistics have been used in several scientific areas. Among them, we can mention works in astrophysics [9], quark-gluon plasma [10], game theory [11], error theory [12], information theory [13], random matrices [14], fractal systems [15], dusty-type plasmas [16], gravitational physics [17,18], epidemiology [19] and reactor physics [5–7,20].

A valuable use of Kaniadakis deformed statistics is in Voigt profile applications. A standard Voigt profile is a probability distribution resulting from the convolution of the Cauchy–Lorentz distribution and the Gaussian distribution. It has been extensively studied in the literature, having applications in a broad spectrum of areas, like astrophysics [21], non-crystalline solids [22], computational and applied mathematics [23], high energy physics [24], applied crystallography [25] and nuclear reactor physics [5–7,20].

However, the standard Voigt profile is only valid for physical systems in thermal equilibrium [2]. With the use of the Kaniadakis distribution, we can consequently obtain a generalized formulation.

In practical applications, the processing time of numerical solutions can be very high due to iterative calculations with a very refined mesh. Thereby, an analytical solution of the same function can save time when inserted into a complex system in the most diverse areas, for example, cross-section data generation for nuclear reactor designs [7,26]. As a consequence, analytical solutions have been continuously studied in the area [27,28].

Hence, this paper presents a novel approach for obtaining an analytical solution for the deformed Voigt profile function using the Kaniadakis distribution.

Also, in this work, we report the computational efficiencies of these two different solutions of the deformed Voigt profile function, numerical and analytical, employing the use of the Kaniadakis distribution. In the reactor physics area, this function is also known as the deformed Doppler broadening function [7,26].

In the next section, the numerical formulation of the deformed Doppler broadening function will be presented using the Kaniadakis distribution. Section 3 describes a new analytical formulation of the same function and Section 4 offers the CPU processing time for both methods and the discussion. Finally, Section 5 presents the conclusions of the paper.

2. Numerical solution for the deformed Voigt profile

Through the Bethe–Placzek approximation, it is possible to present the deformed Doppler broadening function considering the Kaniadakis distribution [5]:

$$\psi_\kappa(\xi,x) = \frac{\xi}{2\sqrt{\pi}}B(\kappa)\int_{-\infty}^{+\infty}\frac{dy}{1+y^2}i\exp_\kappa\left[\frac{-\xi^2(x-y)^2}{4}\right] \tag{6}$$

where:

$$\xi \equiv \frac{\Gamma}{\left(\frac{4E_0k_BT}{A}\right)^{\frac{1}{2}}}; \tag{7}$$

Γ is the total width of the resonance as measured in the laboratory coordinates;
A is the mass number;
E_0 is the resonant energy;

$$y \equiv \frac{2}{\Gamma}(E_{CM}-E_0); \tag{8}$$

E_{CM} is the center-of-mass energy;
E is the energy of the incident neutron;

$$x \equiv \frac{2}{\Gamma}(E-E_0); \tag{9}$$

$$i\exp_\kappa(z) \equiv \frac{\sqrt{1+\kappa^2z^2}-\kappa^2z}{1-\kappa^2}\exp_\kappa(z); \tag{10}$$

$$z = \frac{-\xi^2(x-y)^2}{4} \tag{11}$$

$$B(\kappa) = (2|\kappa|)^{\frac{3}{2}}\left(1+\frac{1}{2}3|\kappa|\right)\frac{\Gamma\left(\frac{1}{2|\kappa|}+\frac{3}{4}\right)}{\Gamma\left(\frac{1}{2|\kappa|}-\frac{3}{4}\right)}. \tag{12}$$

To solve equation (6) numerically, we used Python and Visual Studio code editor.

In nuclear reactor physics applications, we can associate ξ with medium temperature while associating x directly with neutron energy, as represented by equations (7) and (9).

To implement the most efficient numerical solution possible in terms of CPU efficiency, we chose the Simpson method, the most straightforward approach in the literature for obtaining the deformed Doppler broadening function using the Kaniadakis distribution.

Approximating the integrand $f(y)$ of equation (6),

$$f(y) = \frac{1}{1+y^2}i\exp_\kappa\left[\frac{-\xi^2(x-y)^2}{4}\right] \tag{13}$$

with a collection of parabolas subtended across three successive data mesh points, corresponding to a second-degree polynomial, it leads to Simpson's formula, denoted by $S_N(f)$. By using Lagrange's method to construct the polynomial interpolation, the integral of equation (6) may be written as [29]:

$$S_N[f(y)] \cong \frac{\Delta y}{3}\sum_{i=1}^{\frac{N}{2}}[f(y_{2i-2})+4f(y_{2i-1})+f(y_{2i})], \tag{14}$$

where N is an even number of subintervals of $[a,b]$, $\Delta y = (b-a)/N$ and $y_i = a + i\Delta y$ [29]. To obtain the reference values for the numerical solution of ψ_κ [2,3] with less computational time, we assume, in equation (5), $-\infty \to -200$, $+\infty \to 200$, and $N = 1000$ in equation (14) which are the minimum settings to obtain the Benchmark results [7,30]. The precision variance according to the value of N is illustrated in Table 1:

Table 1
Values of N versus the percentage error concerning the Benchmark ($x = 0$ and $\xi = 0.05$).

N	value	% Error	time (s)
300	0.04058	4.67%	155
500	0.04203	1.27%	165
1000	0.04257	0.00%	214
Benchmark	0.04257		

3. Analytical solution for the deformed Doppler broadening function

A recently proposed approximated analytical method for the deformed Doppler broadening function, an alternative to equation (6), was obtained from the proposition of two different methods, depending on their position in the $|x\cdot\xi|$domain. The first one, which we call method 1, and which applies to the domain $|x\cdot\xi|<6$, arises from the proposition of a differential equation and its consequent solution [7]. Method 2, which applies to the $|x\cdot\xi|\geq 6$ domain, arises from performing asymptotic expansions in Taylor series. This paper proposes a new, more robust way to obtain the solution of the homogeneous part of the differential equation obtained for the method.

3.1. A new method for obtaining an analytical solution for $|x\cdot\xi|<6$

One of the ways to obtain an analytical solution for the deformed Doppler broadening function is by finding and solving the following differential equation [6]:

$$\frac{\partial^2\psi_\kappa(\xi,x)}{\partial x^2}+\xi^2 x\frac{\partial\psi_\kappa(\xi,x)}{\partial x}+\frac{\xi^2}{4}\left[2d(\kappa)+\xi^2x^2+\xi^2\right]\psi_\kappa(\xi,x)=\frac{\xi^4}{4}d(\kappa)B(\kappa), \tag{15}$$

which returns to the standard solution, considering the Maxwell–Boltzmann statistics when $\kappa\to 0$:

$$\frac{\partial^2\psi(\xi,x)}{\partial x^2}+\xi^2 x\frac{\partial\psi(\xi,x)}{\partial x}+\frac{\xi^2}{4}\left[2+\xi^2x^2+\xi^2\right]\psi(\xi,x)=\frac{\xi^4}{4}. \tag{16}$$

The solutions for equations (15) and (16) have already been successfully obtained in different papers [6,31,32], using series expansion methods. However, in this paper, we propose an alternative mathematical process: changing the dependent variable to obtain the solution of the homogeneous part of equation (15). Then, we use the traditional parameter variation method to get the same equation's particular solution. Finally, the combination of both techniques results in an analytical solution.

The Frobenius method has already been used in recent works to obtain the solution of the homogeneous part of the differential equation for the deformed Doppler broadening function using the standard Maxwell–Boltzmann distribution [32], as well as in the case of the Kaniadakis distribution [6,7]. However, the application of the Frobenius method makes only sense when solving differential equations with points of regular singularities, which is not the case with differential equations (15) and (16) – even though, in a way, that fact does not invalidate the application of the method to such equations.

Despite being applicable, the use of the Frobenius method to solve the homogeneous part of the differential equations (15) and (16) means that we are forced to hypothetically admit that the homogeneous solution of both equations was proportional to $exp\left(\frac{-\xi^2x^2}{4}\right)$. Therefore, to eliminate the admissibility of such a strong hypothesis, this work proposes an alternative solution for the homogeneous part of equation (15) to eliminate the dependence of the first-order derivative and, thus, reduce the differential equation to the so-called normal form [26].

The homogeneous part of equation (15) can be written without loss of generality as:

$$\frac{d^2}{dx^2}\psi_{\xi,\kappa}(x)+p_\kappa(x)\frac{d}{dx}\psi_{\xi,\kappa}(x)+q_\kappa(x)\psi_{\xi,\kappa}(x)=0, \tag{17}$$

where,

$$p_\kappa(x)\equiv\xi^2 x \tag{18}$$

and

$$q_\kappa(x)\equiv\xi^2\left[2d(\kappa)+\xi^2x^2+\xi^2\right]\Big/4. \tag{19}$$

It is also possible to note that ξ was taken as a parameter so that there is no loss of generality, both in the case of the functions $p_\kappa(x)$and $q_\kappa(x)$ as well as in the case of the ordinary differential equation (ODE) presented in equation (17).

According to Simmons [33], it is possible to represent any differential equation similar to equation (15) by using the dependent variable method, as follows:

$$\frac{d^2}{dx^2}u_{\xi,\kappa}(x)+Q_\kappa(x)u_{\xi,\kappa}(x)=0. \tag{20}$$

The previous equation is also referred to in the literature as the normal form of a second-order homogeneous differential equation [33]. The normal form of equation (17) is achieved by the following steps:

$$\psi_{\xi,\kappa}(x)=u_{\xi,\kappa}(x)v_{\xi,\kappa}(x), \tag{21}$$

so that:

$$\frac{d}{dx}\psi_{\xi,\kappa}(x)=v_{\xi,\kappa}(x)\frac{d}{dx}u_{\xi,\kappa}(x)+u_{\xi,\kappa}(x)\frac{d}{dx}v_{\xi,\kappa}(x) \tag{22}$$

and

$$\frac{d^2}{dx^2}\psi_{\xi,\kappa}(x)=u_{\xi,\kappa}(x)\frac{d^2}{dx^2}v_{\xi,\kappa}(x)+2\frac{d}{dx}u_{\xi,\kappa}(x)\frac{d}{dx}v_{\xi,\kappa}(x)+v_{\xi,\kappa}(x)\frac{d^2}{dx^2}u_{\xi,\kappa}(x) \tag{23}$$

By substituting equations (21)–(23) in the second-order homogeneous differential equation, equation (17), one can obtain the following differential equation, after some algebra [33]:

$$\frac{d^2}{dx^2}u_{\xi,\kappa}(x)+P_\kappa(x)\frac{d}{dx}u_{\xi,\kappa}(x)+Q_\kappa(x)u_{\xi,\kappa}(x)=0, \tag{24}$$

where,

$$P_\kappa(x)\equiv\frac{1}{v_{\xi,\kappa}(x)}\left(2\frac{d}{dx}v_{\xi,\kappa}(x)+p_\kappa(x)v_{\xi,\kappa}(x)\right) \tag{25}$$

and

$$Q_\kappa(x)\equiv\frac{1}{v_{\xi,\kappa}(x)}\left(\frac{d^2}{dx^2}v_{\xi,\kappa}(x)+p(x)\frac{d}{dx}v_{\xi,\kappa}(x)+q_\kappa(x)v_{\xi,\kappa}(x)\right) \tag{26}$$

Equation (25) can be reduced to the normal form by imposing $P_\kappa(x) = 0$ [33]:

$$2\frac{d}{dx}v_{\xi,\kappa}(x) + p_\kappa(x)v_{\xi,\kappa}(x) = 0. \tag{27}$$

Equation (27), in turn, supports the following general solution:

$$v_{\xi,\kappa}(x) = \int \exp\Big(-\xi^2 x/2\Big)dx. \tag{28}$$

Consequently,

$$\frac{d}{dx}v_{\xi,\kappa}(x) = -\frac{1}{2}p_\kappa(x)v_{\xi,\kappa}(x) \tag{29}$$

and

$$\frac{d^2}{dx^2}v_{\xi,\kappa}(x) = \frac{1}{4}p_\kappa(x)^2 v_{\xi,\kappa}(x) - \frac{1}{2}\frac{d}{dx}p_\kappa(x)v_{\xi,\kappa}(x). \tag{30}$$

Note that, from equations (25) and (26), it is possible to show that the term $Q_\kappa(x)$ is exclusively dependent on $p_\kappa(x)$and $q_\kappa(x)$, such that:

$$Q_\kappa(x) = q_\kappa(x) - \frac{p_\kappa(x)^2}{4} - \frac{1}{2}\frac{d}{dx}p_\kappa(x). \tag{31}$$

Therefore, based on the values previously defined for $p_\kappa(x)$ and $q_\kappa(x)$ ($\xi^2 x$ and $\xi^2[2d(\kappa) + \xi^2 x^2 + \xi^2]/4$), the functions $v_{\xi,\kappa}(x)$ and $Q_\kappa(x)$, can be explicitly determined through equations (17) and (27), respectively:

$$v_{\xi,\kappa}(x) = exp\Big(-\frac{\xi^2 x^2}{4}\Big). \tag{32}$$

and

$$Q_\kappa(x) = \frac{\xi^2}{2}d(k) + \frac{\xi^4}{4} - \frac{\xi^2}{2}. \tag{33}$$

Using the definition of $d(k) \equiv 1 - k^2$, equation (33) takes the following simplified form:

$$Q_\kappa = \frac{\xi^4}{4} - \frac{\xi^2 k^2}{2}. \tag{34}$$

Analyzing the term Q_κ, it is possible to notice that it assumes positive and negative values in such a way that:

$$Q_\kappa \geq 0 \;\; when \;\; \xi \geq \sqrt{2}\kappa. \tag{35}$$

$$Q_\kappa \leq 0 \;\; when \;\; \xi \leq \sqrt{2}\kappa. \tag{36}$$

As Q_κ is independent of x, equation (20) therefore presents the following general solution, which can be expressed in two different ways:

$$u_{\xi,\kappa}(x) = \varpi_1 cos\Big(\frac{x}{2}\sqrt{\xi^4 - 2\xi^2\kappa^2}\Big) + \varpi_2 sin\Big(\frac{x}{2}\sqrt{\xi^4 - 2\xi^2\kappa^2}\Big), \tag{37}$$

$$\begin{aligned} u_{\xi,\kappa}(x) =& \varpi_1 exp\Big(\frac{x}{2}\sqrt{-\xi^4 + 2\xi^2\kappa^2}\Big) \\ &+ \varpi_2 exp\Big(-\frac{x}{2}\sqrt{-\xi^4 + 2\xi^2\kappa^2}\Big), \end{aligned} \tag{38}$$

Combining equations (37) and (32), we obtain the solution of the homogeneous part of equation (15), so that:

$$\begin{aligned} \psi_{\xi,\kappa}(x) \equiv \psi_h(\xi,x) =& \exp\Big(\frac{-\xi^2 x^2}{4}\Big) \\ &\times \left\{\varpi_1 cos\Big(\frac{x}{2}\sqrt{\xi^4 - 2\xi^2\kappa^2}\Big) + \varpi_2 sin\Big(\frac{x}{2}\sqrt{\xi^4 - 2\xi^2\kappa^2}\Big)\right\} \end{aligned} \tag{39}$$

From the homogeneous solution, it is possible to find a particular solution using the two linearly independent solutions of equation (37):

$$\psi_1(\xi,x) = \exp\Big(\frac{-\xi^2 x^2}{4}\Big)cos\Big(\frac{x}{2}\sqrt{\xi^4 - 2\xi^2\kappa^2}\Big); \tag{40}$$

$$\psi_2(\xi,x) = \exp\Big(\frac{-\xi^2 x^2}{4}\Big)sin\Big(\frac{x}{2}\sqrt{\xi^4 - 2\xi^2\kappa^2}\Big). \tag{41}$$

By the parameter variation method, it is possible to determine a particular solution, from the linearly independent solutions, equations (40) and (41), as follows:

$$\psi_p(\xi,x) = \mu_1(x)\psi_1(\xi,x) + \mu_2(x)\psi_2(\xi,x), \tag{42}$$

where $\psi_1(\xi,x)$ and $\psi_2(\xi,x)$functions represent linearly independent solutions, equations (40) and (41), and functions $\mu_1(x)$ and $\mu_2(x)$ are determined by the initial conditions.

Following the procedure proposed by the parameter variation method, it is possible to derive:

$$\begin{aligned} \frac{d}{dx}\psi_p =& \frac{d}{dx}\mu_1(x)\psi_1(\xi,x) + \mu_1(x)\frac{d}{dx}\psi_1(\xi,x) + \frac{d}{dx}\mu_2(x)\psi_2(\xi,x) \\ &+ \mu_2(x)\frac{d}{dx}\psi_2(\xi,x). \end{aligned} \tag{43}$$

In order to obtain the new representation of the differential equation, we need to consider $\frac{d}{dx}\mu_1(x)\psi_1(\xi,x) + \frac{d}{dx}\mu_2(x)\psi_2(\xi,x) = 0$ [33], then:

$$\frac{d}{dx}\psi_p = \mu_1(x)\frac{d}{dx}\psi_1(\xi,x) + \mu_2(x)\frac{d}{dx}\psi_2(\xi,x). \tag{44}$$

Differentiating with respect to x, we get the following:

$$\begin{aligned} \frac{d^2}{dx^2}\psi_p =& \frac{d}{dx}\mu_1(x)\frac{d}{dx}\psi_1(\xi,x) + \mu_1(x)\frac{d^2}{dx^2}\psi_1(\xi,x) \\ &+ \frac{d}{dx}\mu_2(x)\frac{d}{dx}\psi_2(\xi,x) + \mu_2(x)\frac{d^2}{dx^2}\psi_2(\xi,x). \end{aligned} \tag{45}$$

By applying the derivatives calculated in equation (15), we get the following:

$$\begin{aligned} &\frac{d}{dx}\mu_1(x)\frac{d}{dx}\psi_1(\xi,x) + \mu_1(x)\frac{d^2}{dx^2}\psi_1(\xi,x) + \frac{d}{dx}\mu_2(x)\frac{d}{dx}\psi_2(\xi,x) \\ &+ \mu_2(x)\frac{d^2}{dx^2}\psi_2(\xi,x) + \xi^2 x\left[\mu_1(x)\frac{d}{dx}\psi_1(\xi,x) + \frac{d}{dx}\mu_2(x)\psi_2(\xi,x)\right] \\ &+ \frac{\xi^2}{4}\Big[2d(\kappa) + \xi^2 x^2 + \xi^2\Big][\mu_1(x)\psi_1(\xi,x) + \mu_2(x)\psi_2(\xi,x)] \\ &= \frac{\xi^4}{4}d(\kappa)B(\kappa). \end{aligned} \tag{46}$$

The functions $\psi_1(\xi,x)$ and $\psi_2(\xi,x)$ are solutions of the associated homogeneous, so that:

$$\frac{d}{dx}\mu_1(x)\frac{d}{dx}\psi_1(\xi,x)+\frac{d}{dx}\mu_2(x)\frac{d}{dx}\psi_2(\xi,x)=\frac{\xi^4}{4}\left(1-\kappa^2\right)B(\kappa). \quad (47)$$

With that, equation (47) and the previous imposition $\frac{d}{dx}\mu_1(x)\psi_1(\xi,x)+\frac{d}{dx}\mu_2(x)\psi_2(\xi,x)=0$, form the following system:

$$\begin{aligned}&\frac{d}{dx}\mu_1(x)\psi_1(\xi,x)+\frac{d}{dx}\mu_2(x)\psi_2(\xi,x)=0\\&\frac{d}{dx}\mu_1(x)\frac{d}{dx}\psi_1(\xi,x)+\frac{d}{dx}\mu_2(x)\frac{d}{dx}\psi_2(\xi,x)=\frac{\xi^4}{4}\left(1-\kappa^2\right)B(\kappa).\end{aligned} \quad (48)$$

This system has a unique solution in $\frac{d}{dx}\mu_1(x)$ and $\frac{d}{dx}\mu_2(x)$, because the Wronskian $W(\psi_1,\psi_2)(x)\neq 0$. The system can be solved by Cramer's rule:

$$\frac{d}{dx}\mu_1(x)=\frac{\begin{vmatrix}0 & \psi_2(\xi,x)\\ g & \frac{d}{dx}\psi_2(\xi,x)\end{vmatrix}}{W(\psi_1,\psi_2)} \quad \text{and} \quad \frac{d}{dx}\mu_2(x)=\frac{\begin{vmatrix}\psi_1(\xi,x) & 0\\ \frac{d}{dx}\psi_1(\xi,x) & g\end{vmatrix}}{W(\psi_1,\psi_2)}, \quad (49)$$

where $g=\frac{\xi^4}{4}(1-\kappa^2)B(\kappa)$. By obtaining $\frac{d}{dx}\psi_1(\xi,x)$, $\frac{d}{dx}\psi_2(\xi,x)$ and calculating $W(\psi_1,\psi_2)$, it is possible to obtain $\frac{d}{dx}\mu_1(x)$ and $\frac{d}{dx}\mu_2(x)$, so that finally these terms are integrated with respect to x. This leads to:

The term $erf(x)$ is the so-called Gaussian error function, defined as follows [34]:

$$erf(x)=\frac{2}{\sqrt{\pi}}\int_0^x e^{-t^2}dt. \quad (52)$$

From that, it is possible to write the particular solution as follows:

$$\psi_p(\xi,x)=\frac{\xi\sqrt{\pi}B(\kappa)}{4}\frac{\sqrt{\xi^4-2\xi^2\kappa^2}}{\xi^2-2\kappa^2}\cdot\exp\left(\frac{\xi^2-2\kappa^2-\xi^2x^2}{4}\right)\times\{i\Omega_1(\xi,x)+\Omega_2(\xi,x)\}, \quad (53)$$

where,

$$\Omega_1(\xi,x)=sin(\Theta)\cdot\Big[-\Big(erf(P_1)\kappa^2-erf(P_1)+erf(P_2)\kappa^2-erf(P_2)\Big)\Big], \quad (54)$$

$$\Omega_2(\xi,x)=cos(\Theta)\cdot\Big[-\Big(2erf(P_3)\kappa^2-2erf(P_3)-erf(P_1)\kappa^2+erf(P_1)+erf(P_2)\kappa^2-erf(P_2)\Big)\Big], \quad (55)$$

$$P_1(\xi,x)=\frac{-i\xi^2x+\sqrt{\xi^4-2\xi^2\kappa^2}}{2\xi} \quad (56)$$

$$\mu_1(x)=\frac{1}{(-\xi^2+2\kappa^2)}\left\{\frac{1}{4}\sqrt{\pi}\cdot\sqrt{\xi^4-2\xi^2\kappa^2}\cdot B(\kappa)\cdot\xi\cdot exp\left(\frac{\xi^2-2\kappa^2}{4}\right)\cdot\begin{bmatrix}2erf\left(\frac{\sqrt{\xi^4-2\xi^2\kappa^2}}{2\xi}\right)\kappa^2-2erf\left(\frac{\sqrt{\xi^4-2\xi^2\kappa^2}}{2\xi}\right)-erf\left(\frac{-i\xi^2x+\sqrt{\xi^4-2\xi^2\kappa^2}}{2\xi}\right)\kappa^2+erf\left(\frac{-i\xi^2x+\sqrt{\xi^4-2\xi^2\kappa^2}}{2\xi}\right)\\+erf\left(\frac{-i\xi^2x-\sqrt{\xi^4-2\xi^2\kappa^2}}{2\xi}\right)\kappa^2-erf\left(\frac{-i\xi^2x-\sqrt{\xi^4-2\xi^2\kappa^2}}{2\xi}\right)\end{bmatrix}\right\} \quad (50)$$

and

$$\mu_2(x)=\frac{i}{(-\xi^2+2\kappa^2)}\left\{\frac{1}{4}\sqrt{\pi}\cdot\sqrt{\xi^4-2\xi^2\kappa^2}\cdot B(\kappa)\cdot\xi\cdot exp\left(\frac{\xi^2-2\kappa^2}{4}\right)\cdot\begin{bmatrix}erf\left(\frac{-i\xi^2x+\sqrt{\xi^4-2\xi^2\kappa^2}}{2\xi}\right)\kappa^2-erf\left(\frac{-i\xi^2x+\sqrt{\xi^4-2\xi^2\kappa^2}}{2\xi}\right)\\+erf\left(\frac{-i\xi^2x-\sqrt{\xi^4-2\xi^2\kappa^2}}{2\xi}\right)\kappa^2-erf\left(\frac{-i\xi^2x-\sqrt{\xi^4-2\xi^2\kappa^2}}{2\xi}\right)\end{bmatrix}\right\}. \quad (51)$$

$$P_2(\xi,x)=\frac{-i\xi^2x-\sqrt{\xi^4-2\xi^2\kappa^2}}{2\xi} \tag{57}$$

$$P_3(\xi,x)=\frac{\sqrt{\xi^4-2\xi^2\kappa^2}}{2\xi} \tag{58}$$

$$\Theta(\xi,x)=\frac{x}{2}\sqrt{\xi^4-2\xi^2\kappa^2} \tag{59}$$

From the general solution obtained by adding the particular and the homogeneous solutions, it is possible to calculate the constants ϖ_1 and ϖ_2 present in the homogeneous solution and, consequently, in the general solution. This calculation is performed by applying the initial conditions:

$$\begin{aligned}\psi_\kappa(\xi,x=0)&=\psi_h(\xi,x=0)+\psi_p(\xi,x=0)=\varpi_1\\&=\frac{\xi}{2\left(1-k^2\right)}\sqrt{\pi}B(\kappa)e^{\frac{\xi^2}{4}}\left[1-\mathrm{erf}\left(\frac{\xi}{2}\right)\right];\end{aligned} \tag{60}$$

$$\begin{aligned}\left.\frac{\partial\psi_\kappa(\xi,x)}{\partial x}\right|_{x=0}&=\left.\frac{\partial\left[\psi_h(\xi,x)+\psi_p(\xi,x)\right]}{\partial x}\right|_{x=0}=\frac{\varpi_2}{2}\sqrt{\xi^4-2\xi^2\kappa^2}\\&=0,\varpi_2=0.\end{aligned} \tag{61}$$

Thus, the following general solution is obtained from the initial conditions:

$$\psi_k(\xi,x)=\exp\left(\frac{\xi^2-\xi^2x^2}{4}\right)\cdot\frac{\xi\sqrt{\pi}B(\kappa)}{4}\left\{D(\xi,x)+\Omega_g(\xi,x)\right\}, \tag{62}$$

where

$$D(\xi,x)\equiv\frac{2-2erf\left(\xi/2\right)}{1-\kappa^2}cos(\Theta) \tag{63}$$

and

$$\Omega_g(\xi,x)\equiv\frac{\sqrt{\xi^4-2\xi^2\kappa^2}}{\xi^2-2\kappa^2}\cdot\exp\left(\frac{-\kappa^2}{2}\right)\left[i\Omega_1(\xi,x)+\Omega_2(\xi,x)\right] \tag{64}$$

An alternative representation of the solution can be obtained by making the following definitions:

$$\Lambda(\xi,x)=\exp\left(\frac{\xi^2-\xi^2x^2}{4}\right)\cdot\frac{\xi\sqrt{\pi}B(\kappa)}{4}; \tag{65}$$

$$\Pi(\xi,x)=\frac{\sqrt{\xi^4-2\xi^2\kappa^2}}{\xi^2-2\kappa^2}\cdot\exp\left(\frac{-\kappa^2}{2}\right); \tag{66}$$

$$\Delta(\xi)=\frac{2-2erf\left(\xi/2\right)}{1-\kappa^2}. \tag{67}$$

Thus, equations (62)–(64) can be expressed by:

$$\psi_k(\xi,x)=\Lambda(x,\xi)\left[D(\xi,x)+\Omega_g(\xi,x)\right], \tag{68}$$

$$D(\xi,x)\equiv\Delta(\xi)\cdot cos(\Theta), \tag{69}$$

$$\Omega_g(\xi,x)\equiv\Pi(x,\xi)\cdot[i\Omega_1(\xi,x)+\Omega_2(\xi,x)]. \tag{70}$$

The analytical solution achieved in this paper is free of approximations and, consequently, satisfies equation (15). Furthermore, by the uniqueness theorem for initial value problems, in the case of second-order differential equations, it can be said that the analytical solution obtained, as shown in equation (68), is unique, as found by Boyce and DiPrima [35] and by Simmons [33].

Another critical point that shows the generality of the obtained solution is the fact that when $\kappa\to0$, the canonical solution proposed by Palma, Martinez and Silva [32] for a standard Voigt profile is reached, such that:

$$\begin{aligned}\lim_{\kappa\to0}\psi_\kappa(\xi,x)=\frac{\xi\sqrt{\pi}}{4}\exp\left(\frac{\xi^2-\xi^2x^2}{4}\right)\cdot\lim_{\kappa\to0}\{&B(\kappa)D(\xi,x)\\&+B(\kappa)\Omega_g(\xi,x)\},\end{aligned} \tag{71}$$

$$\begin{aligned}\lim_{\kappa\to0}\psi_\kappa(\xi,x)=&\frac{\xi\sqrt{\pi}}{2}\exp\left(\frac{\xi^2-\xi^2x^2}{4}\right)\cdot cos\left(\frac{x}{2}\xi^2\right)\\&\left\{1+Re\left(erf\left(\frac{i\xi x-\xi}{2}\right)\right)+\tan\left(\frac{x}{2}\xi^2\right)Im\left(erf\left(\frac{i\xi x-\xi}{2}\right)\right)\right\},\end{aligned} \tag{72}$$

3.2. Analytical solution for $|x\cdot\xi|\geq6$

For the $|x\cdot\xi|\geq6$ domain, a second method is proposed by making an approximation through conducting asymptotic expansions in the Taylor series. From equation (13) one can make the following definition:

$$f_\kappa(x,y)=\frac{1}{1+y^2}\frac{\sqrt{1+\kappa^2\left(\frac{\xi^2}{4}(x-y)^2\right)^2}+\kappa^2\frac{\xi^2}{4}(x-y)^2}{1-\kappa^2} \tag{73}$$

By replacing equation (73) in equation (6), we get:

$$\psi_\kappa(\xi,x)=\frac{\xi}{2\sqrt{\pi}}B(\kappa)\int_{-\infty}^{+\infty}f_\kappa(x,y)\cdot\exp_\kappa\left(-\frac{\xi^2}{4}(x-y)^2\right)dy \tag{74}$$

By expanding function $f_\kappa(x,y)$ in Taylor series at $y=x$, we obtain:

$$\begin{aligned}f_\kappa(y)=&-\frac{1}{(\kappa^2-1)(1+x^2)}+\frac{2x}{(\kappa^2-1)(1+x^2)^2}\cdot(y-x)\\&+\frac{1}{4}\cdot\frac{-\kappa^2\xi^2(1+x^2)^2-12x^2+4}{(\kappa^2-1)(1+x^2)^3}\cdot(y-x)^2+\ldots\end{aligned} \tag{75}$$

The term $\exp_\kappa\left(\frac{-\xi^2(x-y)^2}{4}\right)$ using Taylor series for $y=x$ can be represented by Ref. [7]:

$$\begin{aligned}&\exp_\kappa(z)=\exp\left(\frac{1}{\kappa}\arcsin(\kappa z)\right)=\exp\left(z+\frac{1}{\kappa}\arcsin(\kappa z)-z\right)\\&=\exp(z)\exp\left(\frac{1}{\kappa}\arcsin(\kappa z)-z\right)\approx\exp(z)\exp\left(\frac{\kappa^3z^3}{6}\right)\\&\approx\left(1-\frac{\kappa^3z^3}{6}\right)\exp(z).\end{aligned} \tag{76}$$

Analysing the integrand of equation (74), it is possible to note that it will vanish except in the neighbourhood of $y\sim x$. Therefore,

we may hold up only the first term of expansion (76).

At this point, we make the following definition:

$$h_\kappa(y) = f_\kappa(y)\cdot\exp\left(\frac{-\xi^2(x-y)^2}{4}\right), \tag{77}$$

By rewriting equation (74), we get the following:

$$\psi_\kappa(\xi,x) = \frac{\xi}{2\sqrt{\pi}}B(\kappa)\int_{-\infty}^{+\infty} h_\kappa(y)dy. \tag{78}$$

By integrating equation (77) term by term, we obtain a final expression for the Doppler broadening function, which we called method 2 [7]:

$$\psi_\kappa[\![|x\cdot\xi|\geq 6]\!] \cong B(\kappa)\cdot\left[\frac{1}{(1-\kappa^2)(1+x^2)} + \frac{-3\kappa^2\xi^2-\kappa^2\xi^2x^4+4-12x^2}{2\xi^2(\kappa^2-1)(1+x^2)^3}+\ldots\right] \tag{79}$$

The analytical results for the deformed Doppler broadening function using Kaniadakis distribution considering method 1 and method 2 (five order expansion) are presented in the next section.

Given these two different proposed methods, it is possible to represent the validity of the two methods visually, as can be seen in Fig. 1:

The following section presents the results obtained from the analytical and numerical solutions. Moreover, the processing times of the numerical and analytical solutions under conditions of the same computational methodology were compared.

4. Results and discussion

The calculation of the numerical deformed Doppler broadening function, employing equation (6), can be very computationally costly. There are works in the literature that mention this problem and propose new approaches [36,37]. Hence, using an analytical solution can considerably improve computational modules like FRENDY computer code [36,38].

One of this paper's primary goals was to compare the performance of the numerical and analytical solutions of the deformed Doppler broadening function using the Kaniadakis distribution. To do that, we used the same computational methodology, the *timeit* module from the Python standard library [39], which is constantly applied in the literature for this purpose [40–43]. Our procedure calculates the analytical and numerical deformed Doppler broadening functions for all the mesh points (Fig. 1) one million times each, the default *timeit* settings for the number of repetitions [39], presenting the total CPU value of time for each one hundred points. The numerical and analytical results are shown in Tables 2–5, and the computation times are shown in Tables 6–9.

To simulate the CPU processing time, we computed the solutions one million times for each of the 100 mesh points, requiring a total of one hundred million calculation processes. This order of magnitude is consistent with the actual applications for CPU processing time in most areas. We performed the calculations on a standard PC (8 Gb random access memory, i5-4590T 2.0 GHz maximum frequency).

All the calculated solutions used identical programming languages, compilers and methodology for CPU time calculation, data structure, and the number of executions (10^6 for each point). Thereby, we computed the ratio numerical/analytical between each element of the generated tables and calculated the average of the one hundred results (Tables 10 and 11).

As stated previously, calculating the deformed Doppler

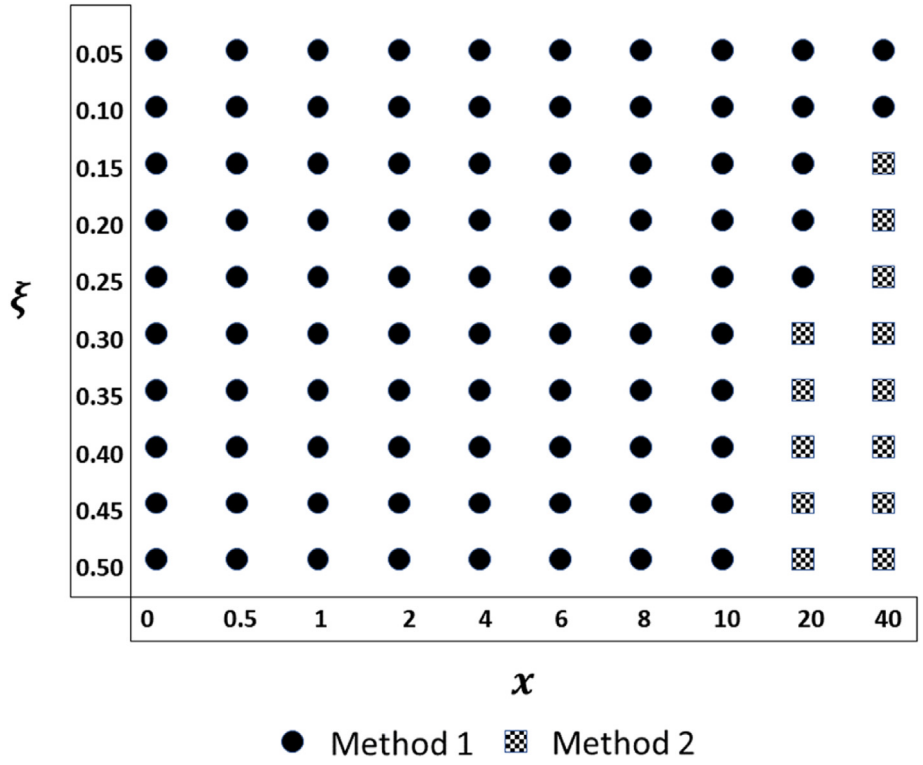

Fig. 1. Representation of the methods validities in the space (x,ξ).

Table 2
Numerical results obtained from equation (5) considering $\kappa = 0.1$

ξ	x = 0	x = 0.5	x = 1	x = 2	x = 4	x = 6	x = 8	x = 10	x = 20	x = 40
0.05	0.04258	0.04257	0.04255	0.04248	0.04217	0.04167	0.04097	0.04010	0.03349	0.01645
0.10	0.08286	0.08281	0.08267	0.08209	0.07982	0.07618	0.07136	0.06563	0.03302	0.00296
0.15	0.12099	0.12084	0.12037	0.11854	0.11149	0.10070	0.08739	0.07294	0.01760	0.00085
0.20	0.15710	0.15676	0.15572	0.15165	0.13644	0.11455	0.08996	0.06632	0.00776	0.00070
0.25	0.19133	0.19068	0.18877	0.18132	0.15451	0.11879	0.08296	0.05326	0.00427	0.00067
0.30	0.22377	0.22272	0.21960	0.20758	0.16609	0.11558	0.07114	0.03992	0.00326	0.00065
0.35	0.25455	0.25297	0.24829	0.23048	0.17193	0.10748	0.05839	0.02938	0.00294	0.00065
0.40	0.28377	0.28153	0.27493	0.25016	0.17297	0.09686	0.04705	0.02221	0.00280	0.00064
0.45	0.31151	0.30849	0.29961	0.26681	0.17026	0.08560	0.03810	0.01775	0.00272	0.00064
0.50	0.33788	0.33394	0.32244	0.28062	0.16483	0.07494	0.03155	0.01510	0.00267	0.00063

Table 3
Numerical results obtained from equation (5) considering $\kappa = 0.2$

ξ	x = 0	x = 0.5	x = 1	x = 2	x = 4	x = 6	x = 8	x = 10	x = 20	x = 40
0.05	0.04098	0.04097	0.04095	0.04088	0.04060	0.04013	0.03948	0.03866	0.03250	0.01658
0.10	0.07979	0.07974	0.07961	0.07907	0.07695	0.07355	0.06906	0.06372	0.03324	0.00402
0.15	0.11657	0.11643	0.11600	0.11429	0.10771	0.09764	0.08522	0.07172	0.01944	0.00117
0.20	0.15145	0.15113	0.15016	0.14636	0.13217	0.11174	0.08875	0.06660	0.00975	0.00078
0.25	0.18455	0.18395	0.18217	0.17522	0.15018	0.11681	0.08324	0.05519	0.00555	0.00069
0.30	0.21597	0.21499	0.21208	0.20085	0.16211	0.11484	0.07299	0.04305	0.00393	0.00066
0.35	0.24581	0.24434	0.23997	0.22334	0.16862	0.10817	0.06152	0.03300	0.00328	0.00065
0.40	0.27418	0.27209	0.26592	0.24279	0.17059	0.09895	0.05099	0.02571	0.00298	0.00064
0.45	0.30115	0.29833	0.29003	0.25938	0.16899	0.08889	0.04232	0.02077	0.00283	0.00064
0.50	0.32681	0.32313	0.31238	0.27330	0.16475	0.07912	0.03563	0.01752	0.00274	0.00064

Table 4
Analytical results obtained from the combination of methods 1 and 2 considering $\kappa = 0.1$

ξ	x = 0	x = 0.5	x = 1	x = 2	x = 4	x = 6	x = 8	x = 10	x = 20	x = 40
0.05	0.04257	0.04256	0.04255	0.04247	0.04216	0.04166	0.04096	0.04009	0.03347	0.01634
0.10	0.08283	0.08278	0.08264	0.08206	0.07978	0.07614	0.07132	0.06557	0.03278	0.00263
0.15	0.12092	0.12077	0.12030	0.11847	0.11141	0.10059	0.08724	0.07271	0.01696	0.00076
0.20	0.15698	0.15664	0.15560	0.15152	0.13627	0.11431	0.08957	0.06576	0.00708	0.00069
0.25	0.19114	0.19050	0.18858	0.18112	0.15422	0.11831	0.08222	0.05227	0.00333	0.00066
0.30	0.22352	0.22247	0.21934	0.20727	0.16561	0.11477	0.06997	0.03857	0.00301	0.00065
0.35	0.25422	0.25263	0.24793	0.23005	0.17118	0.10625	0.05681	0.02786	0.00285	0.00064
0.40	0.28334	0.28110	0.27447	0.24958	0.17189	0.09519	0.04520	0.02075	0.00275	0.00064
0.45	0.31099	0.30795	0.29903	0.26604	0.16879	0.08350	0.03614	0.01649	0.00269	0.00063
0.50	0.33725	0.33329	0.32172	0.27962	0.16291	0.07250	0.02965	0.01407	0.00265	0.00063

Table 5
Analytical results obtained from the combination of methods 1 and 2 considering $\kappa = 0.2$

ξ	x = 0	x = 0.5	x = 1	x = 2	x = 4	x = 6	x = 8	x = 10	x = 20	x = 40
0.05	0.04094	0.04094	0.04092	0.04085	0.04056	0.04009	0.03944	0.03862	0.03242	0.01614
0.10	0.07966	0.07962	0.07948	0.07894	0.07682	0.07340	0.06888	0.06348	0.03229	0.00266
0.15	0.11630	0.11616	0.11572	0.11400	0.10739	0.09722	0.08462	0.07084	0.01693	0.00076
0.20	0.15099	0.15066	0.14969	0.14586	0.13153	0.11079	0.08728	0.06446	0.00693	0.00068
0.25	0.18384	0.18324	0.18144	0.17442	0.14905	0.11497	0.08039	0.05138	0.00344	0.00066
0.30	0.21498	0.21399	0.21104	0.19968	0.16025	0.11172	0.06846	0.03776	0.00298	0.00064
0.35	0.24450	0.24301	0.23858	0.22168	0.16576	0.10344	0.05538	0.02694	0.00282	0.00063
0.40	0.27252	0.27039	0.26412	0.24054	0.16646	0.09246	0.04367	0.01969	0.00272	0.00063
0.45	0.29911	0.29623	0.28776	0.25640	0.16331	0.08072	0.03447	0.01535	0.00266	0.00063
0.50	0.32436	0.32060	0.30958	0.26944	0.15732	0.06958	0.02786	0.01292	0.00262	0.00062

broadening function and, consequently, the quantities that depend on it (like nuclear cross-sections) can be very costly from a computational point of view. Specifically, equation (6) calculation in different applications takes considerable computational time due to the iterative calculations with very narrow meshes.

Hence, in order to overcome this difficulty, we propose an alternative analytical solution considering two different methods for the $|x\cdot\xi|$ space. For the $|x\cdot\xi| < 6$ regions, we presented, in this paper, a new method for solving equation (15). Also, in this work, we introduced the final solution in an alternative, shorter way represented by equation (68). This new formulation is a more robust way to obtain the analytical solution since this method does not require any hypothetical assumptions.

Furthermore, the present work conducted a comparison of CPU

Table 6
Computational times (s) for the numerical results, considering $\kappa = 0.1$.

ξ	x = 0	x = 0.5	x = 1	x = 2	x = 4	x = 6	x = 8	x = 10	x = 20	x = 40
0.05	214.2	194.9	193.6	194.5	197.5	198.2	198.4	196.3	198.5	198.3
0.10	236.1	200.4	188.2	191.9	193.4	192.9	195.5	194.3	191.2	193.0
0.15	195.6	191.0	189.3	190.7	193.0	193.4	195.7	193.4	192.8	195.7
0.20	188.8	191.7	199.2	194.1	198.1	193.6	193.7	193.3	191.8	196.4
0.25	187.4	189.8	205.8	192.7	193.1	190.6	191.8	192.5	192.5	196.9
0.30	190.3	193.3	195.2	193.2	197.1	192.9	190.3	189.8	194.0	193.7
0.35	191.5	212.6	196.4	192.9	192.7	193.9	192.2	192.3	202.0	198.3
0.40	198.9	194.0	190.8	193.6	193.2	196.8	191.6	191.8	197.6	194.6
0.45	198.5	189.2	192.5	191.5	189.3	192.1	189.0	192.0	195.6	196.1
0.50	201.1	187.4	195.0	192.1	194.2	196.6	194.1	193.5	194.9	195.5

Table 7
Computational times (s) for the numerical results, considering $\kappa = 0.2$.

ξ	x = 0	x = 0.5	x = 1	x = 2	x = 4	x = 6	x = 8	x = 10	x = 20	x = 40
0.05	198.1	202.1	200.3	217.5	197.5	199.0	197.0	198.4	196.6	197.2
0.10	190.0	193.1	194.7	202.3	194.3	195.6	192.5	194.4	194.8	195.6
0.15	189.7	193.3	193.7	195.1	193.8	192.9	193.7	195.8	190.7	191.8
0.20	190.9	193.0	206.2	194.6	194.7	192.8	191.5	192.8	198.2	198.3
0.25	189.2	194.8	195.1	193.6	191.9	193.8	196.4	191.6	191.7	193.7
0.30	193.7	198.0	213.4	196.2	199.9	193.4	191.6	195.3	194.4	196.2
0.35	190.8	193.1	215.3	190.7	194.5	195.6	192.7	194.1	193.9	190.9
0.40	193.5	195.8	198.8	197.6	195.3	191.8	194.8	193.0	194.7	197.6
0.45	189.4	194.3	192.2	191.4	191.5	193.3	194.5	191.3	192.8	192.4
0.50	195.7	192.0	196.1	192.4	194.0	193.7	190.7	195.8	195.5	194.4

Table 8
Computational times (s) from the combination of methods 1 and 2 results, considering $\kappa = 0.1$.

ξ	x = 0	x = 0.5	x = 1	x = 2	x = 4	x = 6	x = 8	x = 10	x = 20	x = 40
0.05	36.9	35.6	38.2	38.7	37.5	37.0	38.2	38.2	37.6	38.1
0.10	36.8	37.5	38.4	38.8	38.6	37.4	37.6	36.7	39.0	37.8
0.15	35.2	37.7	37.8	39.1	37.8	39.7	39.8	39.3	40.4	141.1
0.20	35.6	38.5	37.9	38.8	39.0	38.9	38.5	39.4	38.8	136.5
0.25	34.3	37.3	39.7	39.9	40.6	40.4	37.8	38.3	39.4	139.4
0.30	34.2	38.3	38.5	38.5	38.6	38.9	39.2	40.6	143.9	141.7
0.35	35.0	40.1	38.9	41.3	39.1	37.7	38.2	39.5	139.8	138.7
0.40	34.8	40.1	38.3	39.0	40.5	40.0	40.2	40.1	140.0	141.1
0.45	34.8	39.2	39.7	39.0	38.8	39.7	41.2	39.7	141.3	141.5
0.50	36.5	38.6	41.0	39.5	40.4	39.9	40.5	39.5	138.7	140.5

Table 9
Computational times (s) from the combination of methods 1 and 2, considering $\kappa = 0.2$.

ξ	x = 0	x = 0.5	x = 1	x = 2	x = 4	x = 6	x = 8	x = 10	x = 20	x = 40
0.05	37.9	35.6	36.7	37.5	37.6	37.5	38.2	39.3	37.5	37.7
0.10	36.8	40.1	39.0	36.9	38.5	38.5	36.9	46.1	38.2	37.8
0.15	67.0	37.4	39.5	37.3	37.8	38.1	38.3	41.9	38.5	138.9
0.20	37.7	38.6	37.9	39.1	37.3	37.5	37.1	38.6	37.8	135.8
0.25	37.7	38.4	38.2	37.0	38.7	38.7	37.7	37.3	37.4	138.4
0.30	36.4	39.6	38.8	39.5	39.7	39.5	40.3	38.9	142.4	138.3
0.35	35.7	39.0	38.9	38.4	45.5	38.8	37.9	39.4	139.5	137.6
0.40	34.2	39.9	40.4	37.6	40.8	45.7	39.7	41.0	140.9	137.8
0.45	36.1	38.6	39.1	39.3	39.5	48.3	39.9	39.3	142.2	139.7
0.50	35.1	41.6	39.5	38.9	38.5	44.3	39.4	39.2	139.6	140.2

Table 10
Ratio of the numerical/analytical computational times (s) for $\kappa = 0.1$ and the average value.

ξ	x = 0	x = 0.5	x = 1	x = 2	x = 4	x = 6	x = 8	x = 10	x = 20	x = 40
0.05	5.8	5.5	5.1	5.0	5.3	5.4	5.2	5.1	5.3	5.2
0.10	6.4	5.3	4.9	5.0	5.0	5.2	5.2	5.3	4.9	5.1
0.15	5.6	5.1	5.0	4.9	5.1	4.9	4.9	4.9	4.8	1.4
0.20	5.3	5.0	5.3	5.0	5.1	5.0	5.0	4.9	4.9	1.4
0.25	5.5	5.1	5.2	4.8	4.8	4.7	5.1	5.0	4.9	1.4
0.30	5.6	5.1	5.1	5.0	5.1	5.0	4.8	4.7	1.3	1.4
0.35	5.5	5.3	5.0	4.7	4.9	5.1	5.0	4.9	1.4	1.4
0.40	5.7	4.8	5.0	5.0	4.8	4.9	4.8	4.8	1.4	1.4
0.45	5.7	4.8	4.8	4.9	4.9	4.8	4.6	4.8	1.4	1.4
0.50	5.5	4.8	4.8	4.9	4.8	4.9	4.8	4.9	1.4	1.4
									Av.	4.6

Table 11
Ratio of the numerical/analytical computational times (s) for $\kappa = 0.2$ and the average value.

ξ	x = 0	x = 0.5	x = 1	x = 2	x = 4	x = 6	x = 8	x = 10	x = 20	x = 40
0.05	5.2	5.7	5.5	5.8	5.3	5.3	5.2	5.0	5.2	5.2
0.10	5.2	4.8	5.0	5.5	5.0	5.1	5.2	4.2	5.1	5.2
0.15	2.8	5.2	4.9	5.2	5.1	5.1	5.1	4.7	5.0	1.4
0.20	5.1	5.0	5.4	5.0	5.2	5.1	5.2	5.0	5.2	1.5
0.25	5.0	5.1	5.1	5.2	5.0	5.0	5.2	5.1	5.1	1.4
0.30	5.3	5.0	5.5	5.0	5.0	4.9	4.8	5.0	1.4	1.4
0.35	5.3	4.9	5.5	5.0	4.3	5.0	5.1	4.9	1.4	1.4
0.40	5.6	4.9	4.9	5.3	4.8	4.2	4.9	4.7	1.4	1.4
0.45	5.3	5.0	4.9	4.9	4.9	4.0	4.9	4.9	1.4	1.4
0.50	5.6	4.6	5.0	5.0	5.0	4.4	4.8	5.0	1.4	1.4
									Av.	4.6

processing times between the analytical and numerical representations of the deformed Doppler broadening function using the Kadaniadakis distribution.

In this comparison, we found that the analytical solution is approximately 4.6 times faster than the numerical method for both $\kappa = 0.1$ and $\kappa = 0.2$.

5. Conclusions

This paper presents a new approach for solving the differential equation of the analytical Kaniadakis Doppler broadening (KDB) function. By using this methodology, one can solve the homogeneous part of the equation without assuming any approximations, thus advancing over previous solutions presented in recent papers.

Furthermore, for the first time, we present a comparison of computational times between the analytical and numerical solutions for ψ_κ. This comparison emphasizes the potential advantages of using analytical solutions for cases with very costly computational processes. These results show an improvement in efficiency using the analytical approximation, indicating that it may be helpful in different applications that require the calculation of the deformed Voigt function or the deformed Voigt profile in other areas.

Funding

Funding was received for this work.

All the sources of funding for the work described in this publication are acknowledged below:

Coordenação de Aperfeiçoamento de Pessoal de Nível Superior (CAPES).

Conselho Nacional de Desenvolvimento Científico e Tecnológico (CNPq).

Declaration of competing interest

The authors declare that they have no known competing financial interests or personal relationships that could have appeared to influence the work reported in this paper.

Acknowledgment

This study was financed in part by the Conselho Nacional de Desenvolvimento Científico e Tecnológico (CNPq). The authors also thank Coordenação de Aperfeiçoamento de Pessoal de Nível Superior (CAPES) for support through the Procad-Defesa program, professor Su Jian, Kieran Nelson for his proofreading service and the reviewers for their thoughtful comments and efforts towards improving our manuscript.

References

[1] E.T. Jaynes, Information theory and statistical mechanics, Phys. Rev. 106 (1957) 620–630, https://doi.org/10.1103/PhysRev.106.620.
[2] G. Kaniadakis, Statistical mechanics in the context of special relativity. II, Phys. Rev. E 72 (2005), 036108, https://doi.org/10.1103/PhysRevE.72.036108.
[3] G. Kaniadakis, Statistical mechanics in the context of special relativity, Phys. Rev. E 66 (2002), 056125, https://doi.org/10.1103/PhysRevE.66.056125.
[4] G. Kaniadakis, Non-linear kinetics underlying generalized statistics, Phys A Stat Mech Its Appl 296 (2001) 405–425, https://doi.org/10.1016/S0378-4371(01)00184-4.
[5] G. Guedes, A.C. Gonçalves, D.A. Palma, The Doppler broadening function using the kaniadakis distribution, Ann. Nucl. Energy 110 (2017) 453–458, https://doi.org/10.1016/j.anucene.2017.06.057.
[6] W.V. de Abreu, A.C. Gonçalves, A.S. Martinez, Analytical solution for the Doppler broadening function using the Kaniadakis distribution, Ann. Nucl. Energy 126 (2019) 262–268, https://doi.org/10.1016/j.anucene.2018.11.023.
[7] W.V. de Abreu, A.C. Gonçalves, A.S. Martinez, New analytical formulations for the Doppler broadening function and interference term based on Kaniadakis distributions, Ann. Nucl. Energy 135 (2020), 106960, https://doi.org/10.1016/j.anucene.2019.106960.
[8] P.-H. Chavanis, Generalized thermodynamics and Fokker-Planck equations:

applications to stellar dynamics and two-dimensional turbulence, Phys. Rev. E 68 (2003), 036108, https://doi.org/10.1103/PhysRevE.68.036108.
[9] J.C. Carvalho, R. Silva, J.D. do Nascimento jr., B.B. Soares, J.R. De Medeiros, Observational measurement of open stellar clusters: a test of Kaniadakis and Tsallis statistics, EPL (Europhysics Lett 91 (2010) 69002, https://doi.org/10.1209/0295-5075/91/69002.
[10] A.M. Teweldeberhan, H.G. Miller, R. Tegen, κ-deformed statistics and the formation of a quark-gluon plasma, Int. J. Mod. Phys. E 12 (2003) 669–673, https://doi.org/10.1142/S021830130300148X.
[11] F. Topsøe, Entropy and equilibrium via games of complexity, Phys A Stat Mech Its Appl 340 (2004) 11–31, https://doi.org/10.1016/j.physa.2004.03.073.
[12] T. Wada, H. Suyari, κ-generalization of Gauss' law of error, Phys. Lett. 348 (2006) 89–93, https://doi.org/10.1016/j.physleta.2005.08.086.
[13] T. Wada, H. Suyari, A two-parameter generalization of Shannon–Khinchin axioms and the uniqueness theorem, Phys. Lett. 368 (2007) 199–205, https://doi.org/10.1016/j.physleta.2007.04.009.
[14] A.Y. Abul-Magd, Non-extensive random-matrix theory based on Kaniadakis entropy, Phys. Lett. 361 (2007) 450–454, https://doi.org/10.1016/j.physleta.2006.09.080.
[15] A.I. Olemskoi, V.O. Kharchenko, V.N. Borisyuk, Multifractal spectrum of phase space related to generalized thermostatistics, Phys A Stat Mech Its Appl 387 (2008) 1895–1906, https://doi.org/10.1016/j.physa.2007.11.045.
[16] I. Lourek, M. Tribeche, Dust charging current in non equilibrium dusty plasma in the context of Kaniadakis generalization, Phys A Stat Mech Its Appl 517 (2019) 522–529, https://doi.org/10.1016/j.physa.2018.11.008.
[17] E.M.C. Abreu, J.A. Neto, E.M. Barboza, R.C. Nunes, Tsallis and Kaniadakis statistics from the viewpoint of entropic gravity formalism, Int J Mod Phys A 32 (2017), 1750028, https://doi.org/10.1142/S0217751X17500282.
[18] E.M.C. Abreu, J.A. Neto, A.C.R. Mendes, A. Bonilla, R.M. de Paula, Cosmological considerations in Kaniadakis statistics, EPL (Europhysics Lett 124 (2018) 30003, https://doi.org/10.1209/0295-5075/124/30003.
[19] G. Kaniadakis, M.M. Baldi, T.S. Deisboeck, G. Grisolia, D.T. Hristopulos, A.M. Scarfone, et al., The κ-statistics approach to epidemiology, Sci. Rep. 10 (2020) 19949, https://doi.org/10.1038/s41598-020-76673-3.
[20] W.V. De Abreu, A.C. Gonçalves, A.S. Martinez, An analytical approximation for the generalized interference term using the kaniadakis distribution, Proc Int Conf Nucl Eng 27 (2019) 1912, https://doi.org/10.1299/jsmeicone.2019.27.1912, 2019.
[21] C.W. Churchill, S.S. Vogt, J.C. Charlton, The physical conditions of intermediate-redshift M[CLC]g[/CLC] [CSC]ii[/CSC] absorbing clouds from Voigt profile Analysis, Astron. J. 125 (2003) 98–115, https://doi.org/10.1086/345513.
[22] D. De Sousa Meneses, G. Gruener, M. Malki, P. Echegut, Causal Voigt profile for modeling reflectivity spectra of glasses, J. Non-Cryst. Solids 351 (2005) 124–129, https://doi.org/10.1016/j.jnoncrysol.2004.09.028.
[23] G. Pagnini, F. Mainardi, Evolution equations for the probabilistic generalization of the Voigt profile function, J. Comput. Appl. Math. 233 (2010) 1590–1595, https://doi.org/10.1016/j.cam.2008.04.040.
[24] R.A. Kycia, S. Jadach, Relativistic Voigt profile for unstable particles in high energy physics, J. Math. Anal. Appl. 463 (2018) 1040–1051, https://doi.org/10.1016/j.jmaa.2018.03.065.
[25] R.B. Von Dreele, S.M. Clarke, J.P.S. Walsh, 'Pink'-beam X-ray powder diffraction profile and its use in Rietveld refinement, J. Appl. Crystallogr. 54 (2021) 3–6, https://doi.org/10.1107/S1600576720014624.
[26] C. Josey, P. Ducru, B. Forget, K. Smith, Windowed multipole for cross section Doppler broadening, J. Comput. Phys. 307 (2016) 715–727, https://doi.org/10.1016/j.jcp.2015.08.013.
[27] S. Esmail, P. Agrawal, S. Aly, A novel analytical approach for advection diffusion equation for radionuclide release from an area source, Nucl Eng Technol 52 (2020) 819–826, https://doi.org/10.1016/j.net.2019.09.018.
[28] J.C. Jo, J.-J. Jeong, F.J. Moody, Numerical and analytical predictions of nuclear steam generator secondary side flow field during blowdown due to a feedwater line break, Nucl Eng Technol 53 (2021) 1029–1040, https://doi.org/10.1016/j.net.2020.08.022.
[29] P. Walls, Simpson's Rule, Univ Br Columbia, 2019. https://secure.math.ubc.ca/~pwalls/math-python/integration/simpsons-rule/.
[30] WV de Abreu, Solução analítica da função de alargamento Doppler usando a distribuição de Kaniadakis, Universidade Federal do Rio de Janeiro, 2020, https://doi.org/10.13140/RG.2.2.32080.12802/3.
[31] T.P.R. Campos, A.S. Martinez, The dependence of practical width on temperature, Ann. Nucl. Energy 14 (1987) 241–247, https://doi.org/10.1016/0306-4549(87)90045-4.
[32] D.A. Palma, A.S. Martinez, F.C. Silva, The derivation of the Doppler broadening function using Frobenius method, J. Nucl. Sci. Technol. 43 (2006) 617–622, https://doi.org/10.1080/18811248.2006.9711141.
[33] G.F. Simmons, in: Differential Equations with Applications and Historical Notes, second ed., McGraw=Hill, Inc., New York, 1991.
[34] G.B. Arfken, H.J. Weber, F.H. Harris, in: Mathematical Methods for Physicists, seventh ed., Academic Press, Elesvier, 2013. Waltham.
[35] W.E. Boyce, R.C. DiPrima, Second order linear equations, in: Elem. Differ. Equations Bound. Value Probl, tenth ed., John Wiley & Sons, 2012.
[36] K. Tada, S. Kunieda, Y. Nagaya, Nuclear Data Processing Code FRENDY Version 1, Japan Atomic Energy Agency, 2018, https://doi.org/10.11484/jaea-data-code-2018-014.
[37] D.A.P. Palma, A.D.C. Gonçalves, A.S. Martinez, An alternative analytical formulation for the Voigt function applied to resonant effects in nuclear processes, Nucl Instruments Method. Phys Res Sect A Accel Spectrometers, Detect Assoc Equip 654 (2011) 406–411, https://doi.org/10.1016/j.nima.2011.07.029.
[38] K. Tada, Y. Nagaya, S. Kunieda, K. Suyama, T. Fukahori, FRENDY: a new nuclear data processing system being developed at JAEA, EPJ Web Conf. 146 (2017), 02028, https://doi.org/10.1051/epjconf/201714602028.
[39] Python, Timeit, n.d. https://docs.python.org/3/library/timeit.html.
[40] T. Steininger, M. Greiner, F. Beaujean, T. Enßlin, d2o: a distributed data object for parallel high-performance computing in Python, J Big Data 3 (2016) 17, https://doi.org/10.1186/s40537-016-0052-5.
[41] J.M. Huntenburg, C.J. Steele, P.-L. Bazin, Nighres: processing tools for high-resolution neuroimaging, GigaScience 7 (2018) 1–9, https://doi.org/10.1093/gigascience/giy082.
[42] T. Šolc, M. Mohorčič, C. Fortuna, A methodology for experimental evaluation of signal detection methods in spectrum sensing, PLoS One 13 (2018), e0199550, https://doi.org/10.1371/journal.pone.0199550.
[43] P. Heyken Soares, Zone-based public transport route optimisation in an urban network, Public Transp 13 (2021) 197–231, https://doi.org/10.1007/s12469-020-00242-0.